



**Providing Choice & Value**  
Generic CT and MRI Contrast Agents

**FRESENIUS  
KABI**

**CONTACT REP**

**AJNR**

## **Neuroimaging Features of Neurodegeneration with Brain Iron Accumulation**

M.C. Kruer, N. Boddaert, S.A. Schneider, H. Houlden, K.P. Bhatia, A. Gregory, J.C. Anderson, W.D. Rooney, P. Hogarth and S.J. Hayflick

This information is current as  
of July 22, 2025.

*AJNR Am J Neuroradiol* 2012, 33 (3) 407-414

doi: <https://doi.org/10.3174/ajnr.A2677>

<http://www.ajnr.org/content/33/3/407>

## REVIEW ARTICLE

M.C. Kruer  
N. Boddaert  
S.A. Schneider  
H. Houlden  
K.P. Bhatia  
A. Gregory  
J.C. Anderson  
W.D. Rooney  
P. Hogarth  
S.J. Hayflick



# Neuroimaging Features of Neurodegeneration with Brain Iron Accumulation

**SUMMARY:** NBIA characterizes a class of neurodegenerative diseases that feature a prominent extrapyramidal movement disorder, intellectual deterioration, and a characteristic deposition of iron in the basal ganglia. The diagnosis of NBIA is made on the basis of the combination of representative clinical features along with MR imaging evidence of iron accumulation. In many cases, confirmatory molecular genetic testing is now available as well. A number of new subtypes of NBIA have recently been described, with distinct neuroradiologic and clinical features. This article outlines the known subtypes of NBIA, delineates their clinical and radiographic features, and suggests an algorithm for evaluation.

**ABBREVIATIONS:** ACP = aceruloplasminemia; CNS = central nervous system; FAHN = fatty acid hydroxylase-associated neurodegeneration; INAD = infantile neuroaxonal dystrophy; KRS = Kufo-Rakeb syndrome; NAD = neuroaxonal dystrophy; NBIA = neurodegeneration with brain iron accumulation; NFT = neuroferritinopathy; PKAN = pantothenate kinase-associated neurodegeneration; PLAN = phospholipase-associated neurodegeneration; SENDA = static encephalopathy of childhood with neurodegeneration in adulthood; WSS = Woodhouse-Sakati syndrome

**B**efore the widespread availability of MR imaging, a diagnosis of NBIA could be made only at the time of autopsy. In contrast, current diagnosis is facilitated by evaluation by using both T1- and T2-weighted sequences. As a paramagnetic substance,  $\text{Fe}^{3+}$  catalyzes the nuclear spin relaxation of neighboring water protons. With standard clinical parameters, areas rich in iron appear hypointense on T2-weighted sequences, and isointense on T1 sequences. T2\*-weighted acquisitions (gradient-echo sequences) may accentuate this degree of hypointensity (“blooming”) and may be helpful in

identifying NBIA disorders as may susceptibility-weighted images.<sup>1</sup> In biologic iron-oxides,  $\text{Fe}^{2+}$  typically has fewer unpaired electrons than  $\text{Fe}^{3+}$  and is less effective in quenching T2-weighted signal intensity.<sup>2</sup> Calcium may also appear isointense on T1 and hypointense on T2-weighted sequences, mimicking the appearance of iron. The 2 minerals are readily distinguished by CT, however, because  $\text{Ca}^{2+}$  characteristically appears hyperintense to the surrounding brain parenchyma, while iron is isointense. In addition, iron typically appears markedly hypointense on both standard clinical diffusion-weighted and apparent diffusion coefficient sequences. Other metals that may be deposited in neurodegenerative disorders, such as manganese and copper, have a distinct appearance on T1- and T2-weighted sequences, enabling a heuristic approach to diagnosis based on MR imaging parameters. The characteristics of these metals are summarized in Table 1. Despite the utility of MR imaging in this setting, it does not preclude the need for elemental analysis of neuropathologic specimens; rather, it enables putative diagnosis to be made during life.

The radiographic appearance of the lesions themselves is of prime importance. Iron deposition occurs in multiple sclerosis,<sup>3</sup> human immunodeficiency virus dementia,<sup>4</sup> Freidrich ataxia,<sup>5</sup> and Alzheimer and Parkinson diseases,<sup>6</sup> though to a lesser degree than that seen in NBIA (Fig 1). As a neurometabolic disorder, NBIA leads to an approximately symmetric distribution of iron in key gray matter nuclei that are themselves intrinsically enriched in their iron content in healthy individuals (globus pallidus, substantia nigra, red nucleus, dentate nucleus, putamen, and thalamus).<sup>7</sup> In contrast, although intracranial hemorrhage may lead to T2-weighted hypointensity, the breakdown of heme-containing moieties is unlikely to lead to a symmetric discoloration of the basal ganglia. Instead, it is more likely to lead to a variegated appearance, depending on the stage of the hemorrhage, and to gradually resorb with serial imaging. In some cases, the appearance of striatonigral calcinosis may mimic that of NBIA, and deposition may be remarkably symmetric,<sup>8</sup> making it difficult to distinguish the 2 entities. In such cases, CT may be helpful.

MR imaging scanners with higher magnetic field strengths

Received December 2, 2010; accepted after revision December 8.

From the Departments of Pediatrics, Neurology & Neuroscience, Sanford Children's Research Center, University of South Dakota Sanford College of Medicine (M.C.K.), Sioux Falls, South Dakota; Department of Molecular and Medical Genetics (A.G., P.H., S.J.H.); Division of Neuroradiology (J.C.A.), Department of Radiology; W.M. Keck Foundation High-Field MRI Laboratory, Advanced Imaging Research Center (W.D.R.); Departments of Biomedical Engineering (W.D.R.), Behavioral Neuroscience (W.D.R.), Neurology (P.H.), and Pediatrics (M.C.K., S.J.H.); Oregon Health and Science University, Portland, Oregon; Département de Radiologie Pédiatrique (N.B.), Institut National de la Santé et de la Recherche Médicale U1000, Université Paris Descartes, Hôpital Necker-Enfants Malades, Paris, France; Department of Neurology (S.A.S.), Section of Clinical and Molecular Neurogenetics, University Luebeck, Luebeck, Germany; and Department of Molecular Neuroscience and Reta Lila Weston Institute (H.H.) and Sobell Department of Motor Neuroscience and Movement Disorders (K.P.B.), University College London Institute of Neurology, London, United Kingdom.

M.C.K. is supported by the NBIA Disorders Association and Associazione Italiana Sindromi Neurodegenerative da Accumulo di Ferro, American Academy of Neurology (Clinical Research Training Fellowship), American Philosophical Society, and Medical Research Foundation of Oregon. M.C.K. also receives support through the Oregon Clinical and Translational Research Institute as an OCTRI Scholar (National Center for Research Resources grant UL1 RR024140) and through an National Institutes of Health Loan Repayment Award (UWXY3099). H.H. is supported by the UK Medical Research Council (fellowship, G108/638 and G0802760). S.J.H. is supported by the NBIA Disorders Association. A portion of this work was undertaken at University College of London/University College of London Hospital, which received a proportion of funding from the National Institute for Health Research Biomedical Research Centres funding scheme of the Department of Health.

Please address correspondence to Michael C. Kruer, MD, Departments of Pediatrics, Neurology & Neuroscience, Sanford Children's Research Center, University of South Dakota Sanford College of Medicine, 2301 E. 60th St. North, Sioux Falls, SD 57104; e-mail: michael.kruer@sanfordhealth.org



Indicates open access to non-subscribers at [www.ajnr.org](http://www.ajnr.org)

<http://dx.doi.org/10.3174/ajnr.A2677>

**Table 1: Neuroimaging features of clinically relevant metals**

| Metal            | T <sub>1</sub> Appearance | T <sub>2</sub> Appearance | Other Features   |
|------------------|---------------------------|---------------------------|------------------|
| Ca <sup>2+</sup> | Hypo-/hyperintense        | Hypointense               | Hyperdense on CT |
| Fe <sup>3+</sup> | Isointense                | Hypointense               | Iso-dense on CT  |
| Mn <sup>2+</sup> | Hyperintense              | Isointense                |                  |
| Cu <sup>2+</sup> | Iso-/hyperintense         | Hypo-/hyperintense        |                  |

**Note:**—Mn<sup>2+</sup> indicates manganese ions; Cu<sup>2+</sup>, copper ions.

have increased sensitivity to iron when using T2- and T2\*-weighted acquisitions. This becomes clinically important when comparing 1T or 1.5T scans with those obtained by using 3T magnets. The degree of hypointensity in the globus pallidus and substantia nigra is markedly more robust in 3T magnets.<sup>9</sup> In addition, the degree of hypointensity increases with age, consistent with an age-dependent iron deposition,<sup>10,11</sup> both in normal aging and in NBIA. To correctly identify excess iron clinically, one must thus have a working knowledge of both age- and field-dependent norms. MR imaging techniques that are not yet in widespread clinical use include quantitative T2 mapping sequences, which may be useful in quantifying iron content.<sup>12</sup>

Most interesting, iron deposition detectable by MR imaging may precede the development of clinical symptoms, as evidenced by the identification of an “eye-of-the-tiger” in pre-symptomatic mutation-positive siblings of children affected by PKAN.<sup>13</sup> In contrast, children with INAD may develop iron deposition later in their disease course or not at all.<sup>14</sup> The observation that the degree of iron deposition correlates incompletely with clinical symptoms suggests that though iron is a useful neuroimaging feature in NBIA, it likely is neither necessary nor sufficient to produce the disease phenotype. This has important clinical implications because clinical trials are currently underway for deferiprone, a chelating agent known to traverse the blood-brain barrier.<sup>15</sup> Deferiprone has been shown to reverse iron deposition in Friedreich ataxia, associated with an appreciable decrease in iron content as measured by MR imaging.<sup>12</sup> It remains to be seen whether this agent will have a similar effect in NBIA and whether decreasing the brain iron burden will affect patients’ clinical courses.

### Subtypes of NBIA and Associated Neuroimaging Features

All of the NBIA disorders feature iron deposition in the globus pallidus but differ in the co-occurrence of other findings. They are unified by the clinical constellation of a movement disorder and neurodegenerative course. All are autosomal recessive except for neuroferritinopathy. However, disease onset is variable and may range from early childhood to old age. Clinical features and severity may vary with the age of onset and the nature of the underlying mutation, though genotype-phenotype correlations are incomplete.<sup>14</sup> Idiopathic forms of NBIA, whose responsible genes await identification, may account for up to 40% of cases. An algorithm describing an approach to diagnosis using clinical and neuroimaging features is presented in Fig 2.

### PKAN

PKAN is caused by mutations in *PANK2*.<sup>16</sup> PKAN is the most frequently encountered subtype of NBIA, though still a rare disorder, with an estimated prevalence of ~1:1,000,000. Classic PKAN begins in childhood, with profound dystonia, dys-

arthria, spasticity and pyramidal tract signs, and pigmentary retinopathy, leading to night blindness and visual field constriction. Intellectual deterioration is variable and tends to be more severe in those with earlier disease onset.<sup>17</sup> In later onset atypical forms, dystonia often manifests with prominent orobuccolingual action-induced eating dystonia. Parkinsonism (rigidity, bradykinesia, palilalia, and freezing) and prominent neuropsychiatric features, such as hyperactivity, impulsivity, obsessive-compulsive disorder, and vocal and motor tics, can be seen, as well as depression and anxiety. Seizures and peripheral neuropathy are not typical of PKAN.

MR imaging reveals evidence of iron deposition in the globus pallidus and, to a lesser extent later in the disease, the substantia nigra. In addition, the so-called eye-of-the-tiger sign is virtually pathognomonic of the disorder. The eye-of-the-tiger is produced by a T2-weighted hypointense globus pallidus with a central anteromedial region of T2 hyperintensity (Fig 3). Histopathologically, the “eye” corresponds to a region of profound rarefaction surrounded by relatively more preserved iron-laden neuropil, neurons, and astrocytes.<sup>18</sup> Other forms of NBIA have been purported to exhibit an eye-of-the-tiger<sup>1,19</sup> but feature subtle differences in the appearance of the globus pallidus lesion, including asymmetry, irregular contour, and lateral displacement (Fig 3 versus 4). The central T2-weighted hyperintensity in PKAN may become more intensified with time, appearing to consolidate on serial imaging studies,<sup>20</sup> or it may fade with time.<sup>21</sup> This latter scenario may contribute to some of the cases of PKAN that do not have the typical eye-of-the-tiger appearance.<sup>21</sup> Multiple-system atrophy,<sup>22</sup> cortical basal ganglionic degeneration,<sup>23</sup> multiple sclerosis, and neurofibromatosis may also cause similar-appearing lesions but typically differ in their clinical presentation, course, and/or associated imaging features. Conditions that lead to an eye-of-the-tiger-like appearance in non-NBIA disorders characteristically lack the T2-weighted hypointensity indicative of iron deposition. White matter abnormalities are conspicuously absent in PKAN.

### NAD

Mutations in the gene encoding calcium-independent phospholipase A<sub>2</sub> (*PLA2G6*) lead to NAD,<sup>24</sup> which is subdivided into INAD and later-onset atypical forms. INAD is typified by developmental arrest, then regression of language and motor skills. Affected children are profoundly hypotonic and later develop a progressive spastic quadriplegia with pyramidal dysfunction. Optic atrophy leads to loss of visual acuity and ultimate blindness. Dementia is usually relentlessly progressive. A progressive peripheral neuropathy leads to hyporeflexia. Seizures sometimes occur. Dystonia tends to be milder than that in PKAN but may occur. Ataxia/dysmetria may also be seen. Atypical NAD may present with progressive spasticity, ataxia, and dystonia, along with optic atrophy, peripheral neuropathy, and cognitive impairment.

Radiographically, NAD often features iron deposition in the globus pallidus. The substantia nigra may also be affected. Significant atrophy of both the cerebellar vermis and hemispheres is a frequent feature and typically precedes iron accumulation (Fig 5). Confluent T2 hyperintensities in white matter may be observed, though these are less prominent than in some other forms of NBIA.

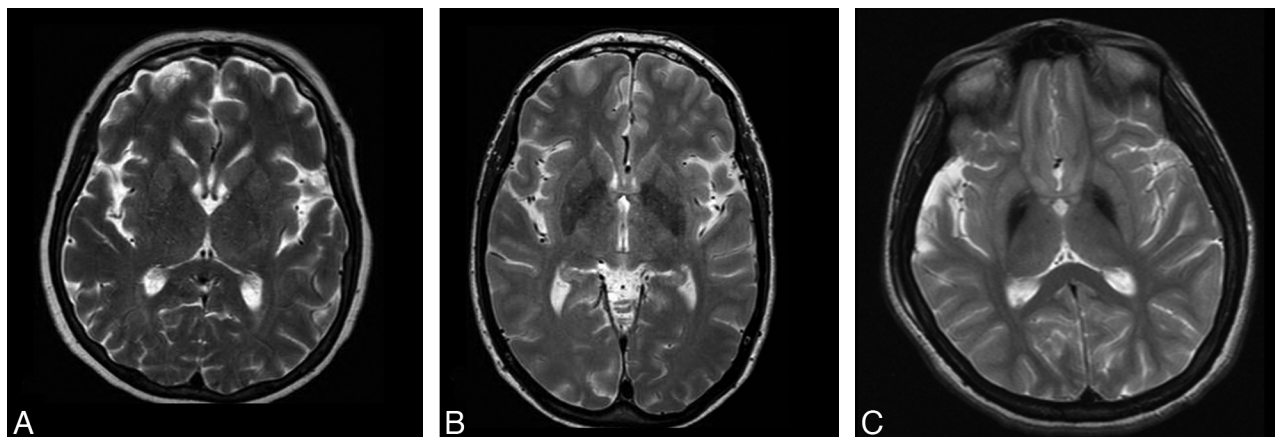


**Fig 1.** T2-weighted MR imaging appearance of a healthy 60-year-old woman (A), a 66-year-old woman with idiopathic Parkinson disease (B), and a 16-year-old female patient with idiopathic NBIA (C) obtained on a 1.5T scanner by using standard clinical TEs and TRs.

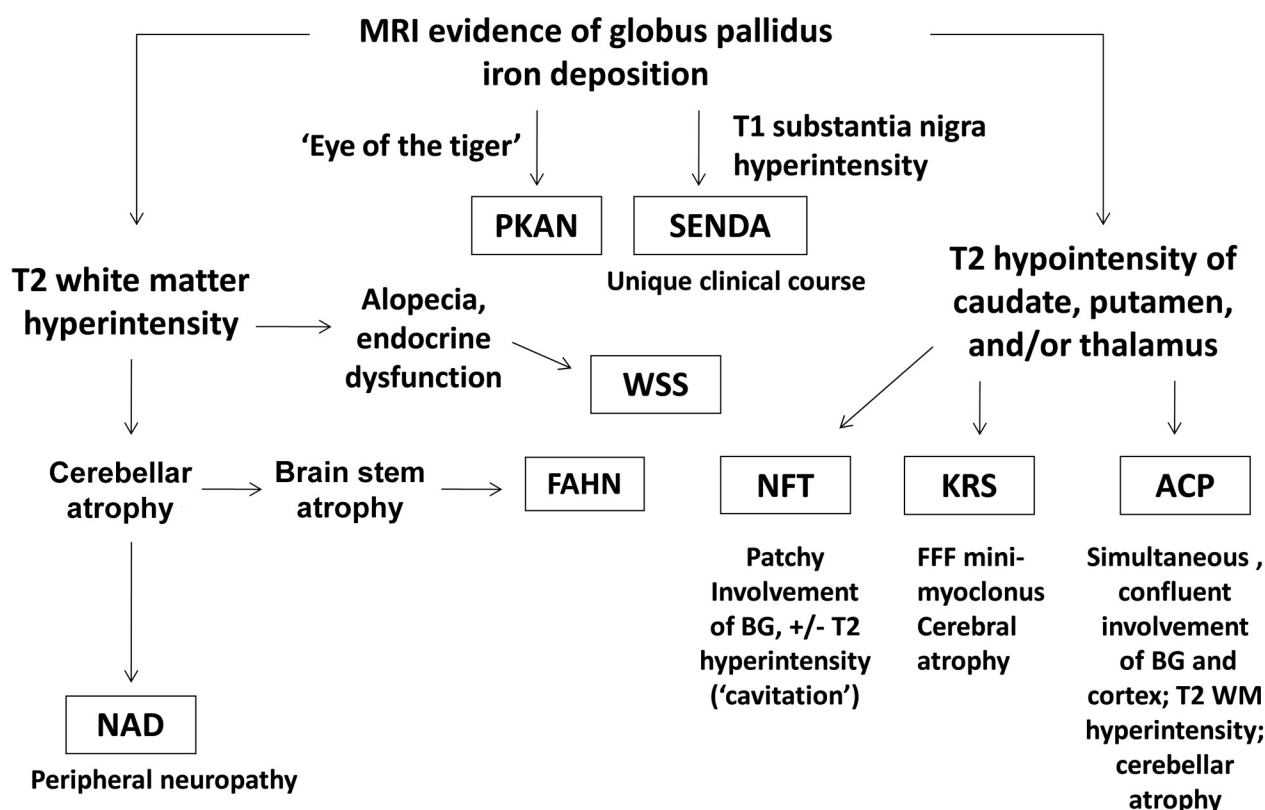


**Fig 2.** A clinical- and neuroimaging-based algorithm for evaluating patients with suspected NBIA. BG indicates basal ganglia; WM, white matter; FFF, facial-faucial-finger

## NFT

A Huntington disease phenocopy,<sup>25</sup> NFT is the only known autosomal dominant form of NBIA and is caused by mutations in the *FTL* gene, leading to ferritin aggregation in the brain and on skin biopsy. Affected patients may present in adolescence to older adulthood. Extraparallel features may be complex, combining parkinsonism, choreoathetosis, dystonia, tremor, and ataxia. Frontal lobe or subcortical dementia often occurs after the onset of motor symptoms, and autonomic features may occur. A supranuclear gaze palsy may be observed. No ophthalmologic findings or seizures are typical. Serum ferritin levels are frequently decreased.<sup>26</sup>

Neuroimaging of NFT may demonstrate high T2 signal

intensity in the basal ganglia early in the course of the disease. This may be mixed with low T2 signal intensity indicative of iron deposition at later stages. However, in general, excess iron deposition becomes evident in the putamen, globus pallidus, and dentate nucleus (Fig 4). The caudate and thalamus may also be involved. Cystic cavitation evolves with time and may be preceded by hyperintense T1-weighted signal intensity, particularly in the putamen and globus pallidus. Mild cerebral and cerebellar atrophy may be seen.

## ACP

Loss of function mutations in the *CP* gene, encoding the protein ceruloplasmin, lead to misregulation of both sys-

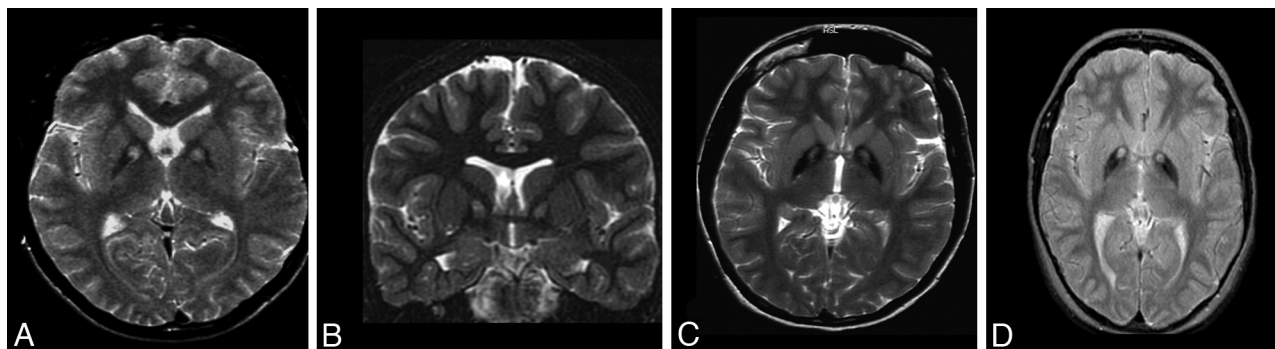


**Fig 3.** PKAN. *A* and *B*, The eye-of-the-tiger sign begins with T2 hyperintensity within the globus pallidus. *C* and *D*, Iron subsequently accumulates with time. Cerebral and/or cerebellar atrophy and white matter hyperintensity are not typical features.

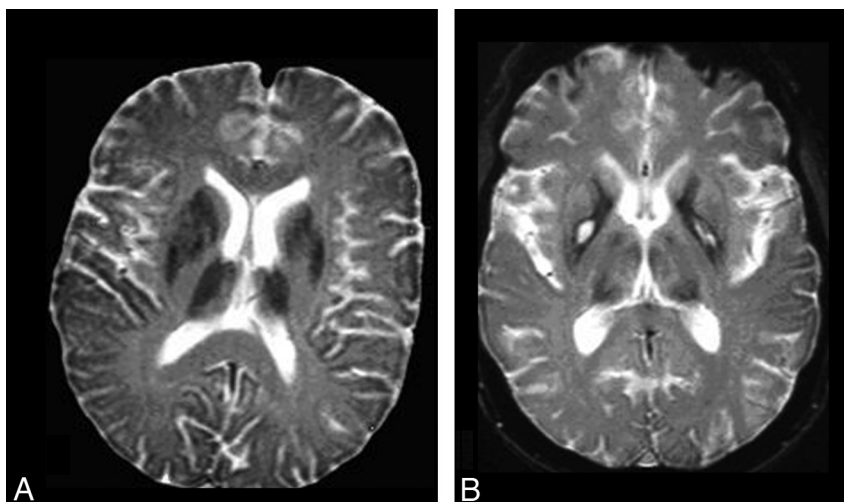


**Fig 4.** NFT. *A*, Patchy hypointensity is typically seen within multiple deep gray nuclei, including the caudate, putamen, globus pallidus, and thalamus in symptomatic cases. *B*, Concurrent T2 hyperintensities (cavitation) may be seen within regions of hypointensity. Images courtesy of P.F. Chinnery.

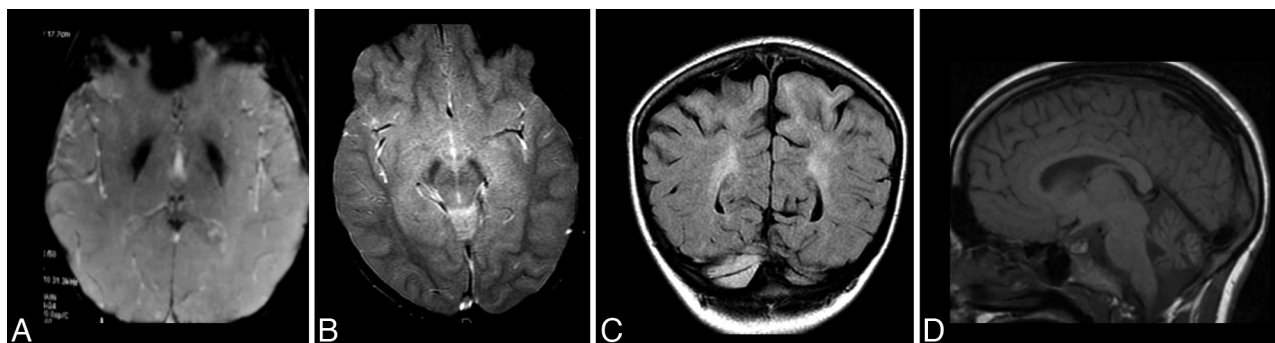


**Fig 5.** NAD. Iron deposition may be seen in the globus pallidus (*A*) and the substantia nigra (*B*) on T2\* and T2 images. *C*, Confluent white matter hyperintensities may be seen on fluid-attenuated inversion recovery sequences as well. *D*, Global cerebellar atrophy is a frequent feature.

temic and CNS iron trafficking because ceruloplasmin is critical for the function of ferroportin, a cellular iron exporter.<sup>27</sup> Ceruloplasmin also has ferroxidase activity, which plays a role in iron mobilization.<sup>28</sup> This leads to both CNS and peripheral iron deposition. ACP mutation-positive individuals typically develop symptoms in mid-adulthood. Clinically, affected patients may have blepharospasm, chorea, craniofacial dyskinesias, ataxia, and retinal degeneration. Diabetes and liver involvement are common complications putatively related to iron deposition in the viscera. T2-weighted hyperintensity in white matter may be prom-

inent. Serum studies typically demonstrate undetectable ceruloplasmin and reduced copper levels and often demonstrate depressed serum iron levels and a microcytic hypochromic anemia as well as elevated ferritin.

Similar to what occurs in NFT but in contrast to most other forms of NBIA, widespread brain iron deposition develops in ACP, with MR imaging evidence of involvement of the caudate, putamen, globus pallidus, thalamus, red nucleus, and dentate (Fig 6). Cerebellar atrophy may also occur as well as hypointensity on T1-weighted imaging in regions of T2 hypointensity.

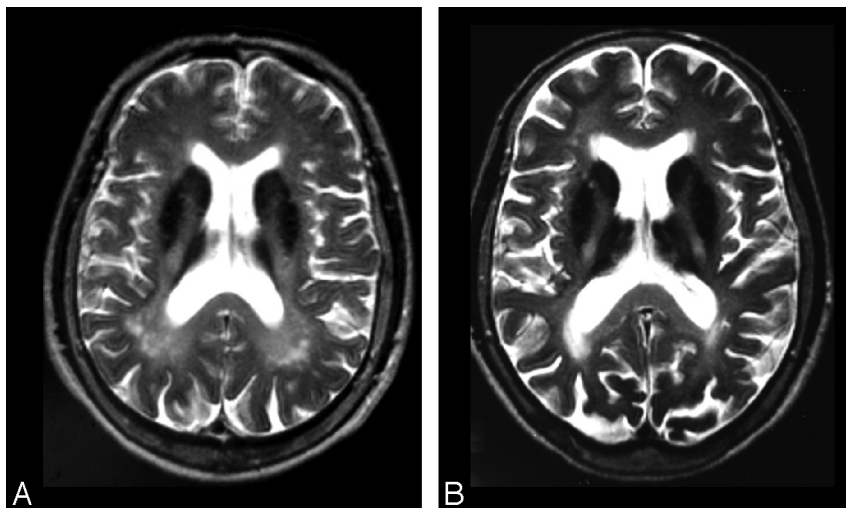


**Fig 6.** ACP. *A* and *B*, More homogeneous iron deposition is seen within the basal ganglia, with juxtapsed confluent white matter hyperintensities on T2-weighted sequences. Images courtesy of H. Miyajima.

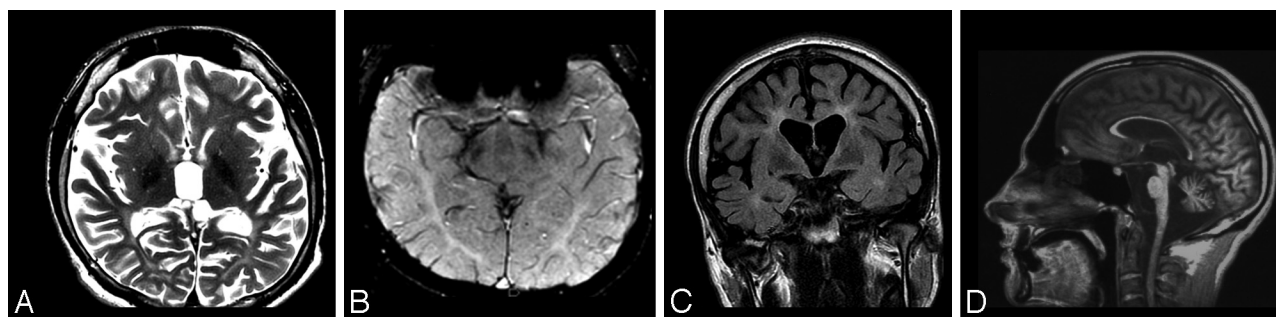


**Fig 7.** FAHN. Evidence of iron deposition in the globus pallidus (*A*) and, to a lesser extent, the substantia nigra (*B*) may be seen on T2-weighted images. *C*, Confluent white matter abnormalities may be apparent on T2/fluid-attenuated inversion recovery sequences. *D*, Mild cerebral atrophy may occur, along with significant pontocerebellar atrophy and thinning of the corpus callosum (*A*).

### FAHN

FAHN is a recently described NBIA subtype caused by mutations in *FA2H*.<sup>29</sup> FAHN typically begins with focal dystonia and gait impairment. Ataxia follows, and dysarthria and progressive spastic quadriparesis with pyramidal tract signs develop. Strabismus and nystagmus may ensue, along with optic atrophy leading to progressive loss of visual acuity. Intellectual performance is variable, and the intellect may be relatively spared in some cases. Seizures may be observed later in the disease course and are typically responsive to anticonvulsants. The disorder is similar in many ways to NAD, except that neither the peripheral neuropathy nor the profound axial hypotonia observed in NAD is a feature.

Neuroimaging features of FAHN include the characteristic presence of iron in the globus pallidus. The substantia nigra may be affected to a lesser degree. Other features include confluent subcortical and periventricular white matter T2 hyperintensities along with thinning of the corpus callosum. Cerebellar and brain stem atrophy increase with time and may be profound (Fig 7).

### KRS

KRS, originally identified as a parkinsonian syndrome, has recently been characterized as a form of NBIA.<sup>30,31</sup> KRS is caused by mutations in the *ATP13A2* gene. Clinical features of KRS include prominent parkinsonism (hypomimia, rigidity,

festination, and bradykinesia), anarthria, spastic paraparesis, and pyramidal tract signs. Dementia is part of the typical constellation of symptoms. Distinguishing features include a supranuclear gaze palsy, oculogyric crises, and facial-faucial-finger minimyoclonus. Aggression and episodes of psychosis, including frank hallucinations, may occur.

Evaluation of MR imaging findings may disclose generalized cerebral, cerebellar, and brain stem atrophy, along with progressive atrophy of the pyramids. Globus pallidus, caudate, and putamen T2 hypointensity justifies consideration as an NBIA disorder (Fig 8).

### WSS

Mutations in *c2orf37*, encoding a nucleolar protein, were recently identified in patients with WSS.<sup>32</sup> Clinically, affected individuals develop progressive dystonia, with or without choreoathetosis. Pyramidal tract involvement is usually not a prominent feature. Peripheral neuropathy may be seen in a subset of patients with WSS. Intellectual impairment is typical and may be progressive. Characteristic phenotypic features include a dysmorphic facial appearance, polyendocrine dysfunction (diabetes mellitus, hypogonadotropic hypogonadism), alopecia, sensorineural hearing loss, and flattened T waves on electrocardiogram. Visual impairment occurs, but in the form of keratoconus. The hypogonadism observed in WSS may also occur in murine models of PKAN.<sup>33</sup>

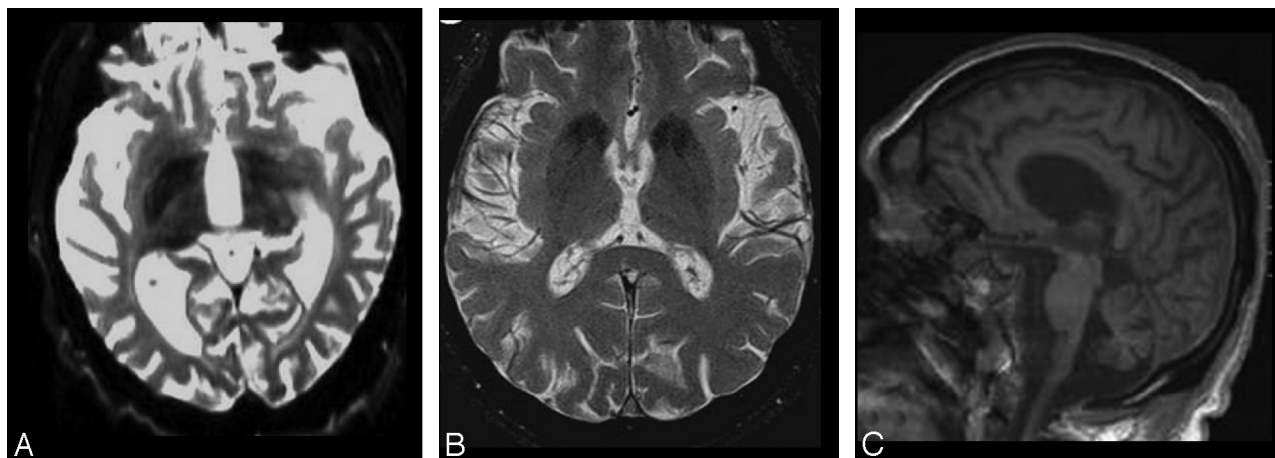


**Fig 8.** KRS. Globus pallidus, caudate, and putamen hypointensity may be seen on T2-weighted images (A and B), in addition to generalized cerebral and cerebellar atrophy (A and C).

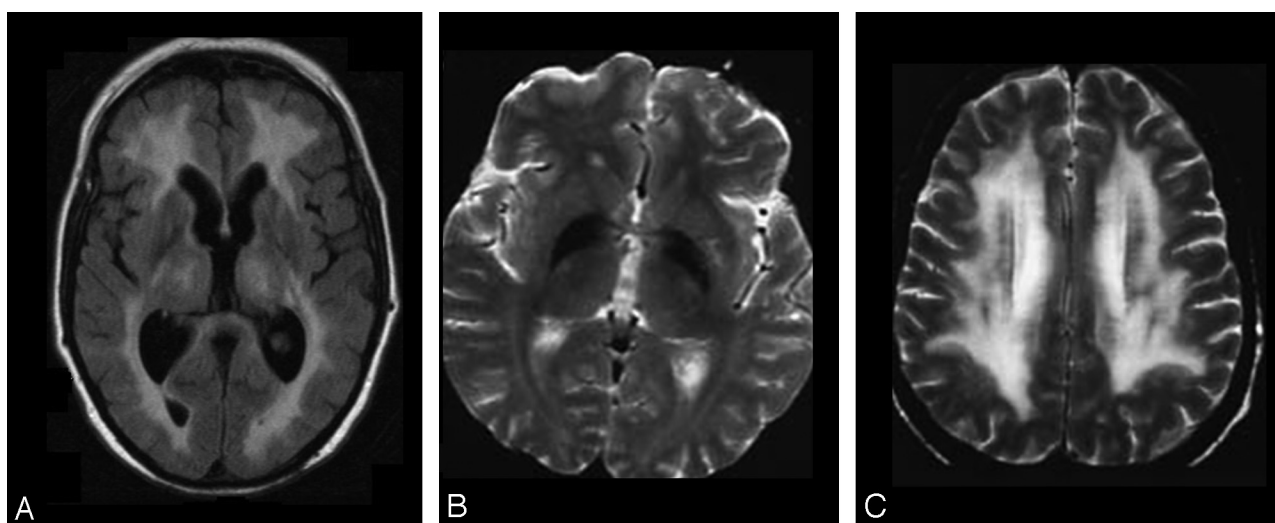


**Fig 9.** WSS. Extensive confluent white matter T2 hyperintensity is typical of the disorder (A and C), while hypointensity of the globus pallidus on T2 sequences is an inconsistent feature (B). Images courtesy of S. Bohlega.

The most atypical of the NBIA disorders, WSS, nevertheless, may feature prominent globus pallidus iron accumulation (Fig 9), though this may be an inconsistent feature. Widespread confluent and marked periventricular T2 white matter hyperintensities are typical findings.

### SENDA

SENDA begins with early childhood intellectual impairment. Unlike the other forms of NBIA, however, the cognitive dysfunction remains nonprogressive, sometimes for decades, after first being recognized. Then, in adulthood, affected patients develop severe dystonia-parkinsonism, and later exhibit signs of a progressive dementia.<sup>34</sup> No etiology has yet been identified for SENDA.

The neuroimaging of SENDA is distinct. In addition to iron deposition in the globus pallidus and substantia nigra, SENDA features T1 hyperintensity of the substantia nigra with a central band of T1 hypointensity (Fig 10). Significant cerebral and milder cerebellar atrophy also occur.

### NBIA Disorders without Iron Deposition

Although NBIA disorders are defined, in part, on the basis of the characteristic deposition of iron in the brain, mutations in NBIA genes may not always lead to iron deposition. Indeed, the phenotype associated with mutations in NBIA genes may be surprisingly diverse,<sup>35</sup> and neuroimaging findings may be similarly variable. For example, iron deposition in NAD may occur later in the disease course or not at all, and a recently identified allelic form of parkinsonism-dystonia is caused by mutations in *PLA2G6*, with onset in adulthood but without iron deposition on neuroimaging.<sup>36</sup> The recognition that mutations in *PLA2G6* do not always lead to a clear NAD phenotype has led investigators to propose the name PLAN to describe the general class of neurodegenerative disorders caused by mutations in this gene.<sup>37</sup>

Although recognizing the phenotypic heterogeneity of NBIA disorders is important, converging evidence implicates several subtypes of NBIA in a shared pathway linking abnormalities of lipid metabolism with fundamental mechanisms underlying neurodegeneration.<sup>29</sup> Given the overlap with other neurodegenerative disorders, improved understanding of

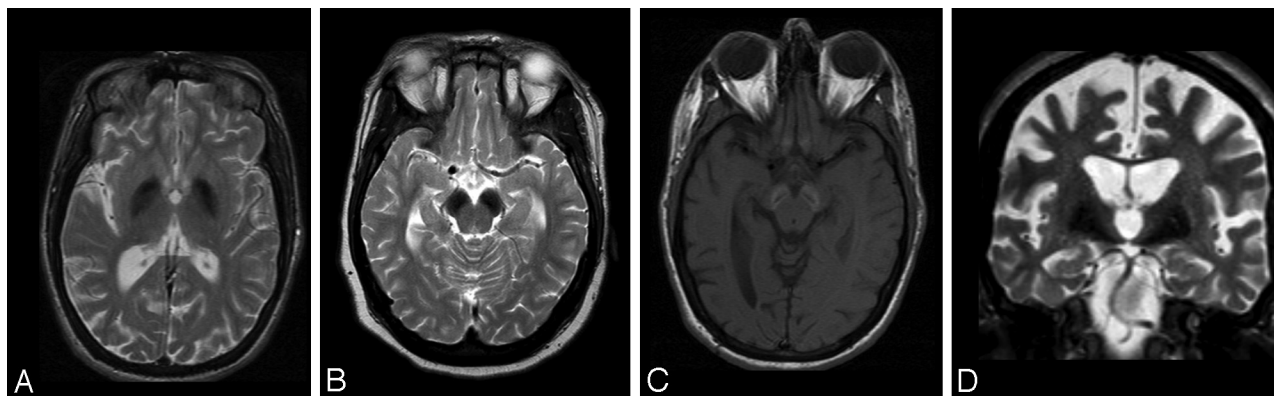


**Fig 10.** SENDA. Hypointensity of the globus pallidus (A) is overshadowed by that of the substantia nigra and cerebral peduncles (B) on T2-weighted imaging. C, T1 sequences demonstrate hyperintensity of the substantia nigra and cerebral peduncles with central linear hypointensity. D, Global cerebral atrophy is also a feature.

**Table 2: Comparison of neuroimaging features in NBIA**

| Disorder | Iron Deposition   | White Matter Involvement | Other Findings                                       |
|----------|---|--------------------------|--|
| PKAN     | Globus pallidus, substantia nigra (mild)                          | No                       | Eye-of-the-tiger sign                                |
| PLAN     | Globus pallidus, <sup>a</sup> substantia nigra <sup>a</sup>       | Mild                     | Moderate cerebellar atrophy                          |
| NFT      | "Patchy" globus pallidus, putamen, caudate, dentate, thalamus     | Mild, moderate           | Cystic cavitation, mild cerebral, cerebellar atrophy |
| ACP      | Globus pallidus, putamen, caudate, thalamus, red nucleus, dentate | Moderate, severe         | Mild cerebellar atrophy                              |
| FAHN     | Globus pallidus, substantia nigra <sup>b</sup>                    | Moderate                 | Pontocerebellar atrophy                              |
| KRS      | Globus pallidus, putamen, caudate <sup>b</sup>                    |                          | Severe cerebral, cerebellar, brain stem atrophy      |
| WSS      | Globus pallidus <sup>b</sup>                                      | Severe, confluent        |  |
| SEDA     | Substantia nigra, globus pallidus                                 | Occasional               | Midbrain T1 hyperintensity                           |

<sup>a</sup> Inconsistent finding.

<sup>b</sup> Numbers of genetically confirmed cases are still too small to determine the frequency of iron deposition.

NBIA may lead to parallel insights into related synucleinopathies and tauopathies.<sup>38–40</sup>

## Conclusions

MR imaging is of tremendous utility in the evaluation of brain iron disorders and facilitates clinical diagnosis. Despite its usefulness as a biomarker, the pathophysiologic role of iron deposition in NBIA remains uncertain. Associated MR imaging abnormalities may help to distinguish subtypes of NBIA and facilitate a more definitive diagnosis (Table 2). New applications of MR imaging in NBIA, including the evaluation of disease evolution in clinical trials and the quantification of iron content in vivo, may facilitate efforts to develop treatments for these devastating diseases.

## Acknowledgments

We acknowledge the graciousness of P.F. Chinnery and H. Miyajima in providing images of NFT and ACP, respectively, and of S. Bohlega in providing images of WSS.

**Disclosures:** Michael C. Kruer, *Research Support (including provision of equipment or materials):* EMD Serono, *Details:* research (grant) support. Henry Houlden: *Research Support (including provision of equipment or materials):* Medical Research Council UK and Wellcome Trust, *Details:* grant support. Kailash Bhatia, *Research Support (including provision of equipment or materials):* Ipsen Ltd, Wellcome Trust, PD Society; Dystonia Society, UK, *Details:* research unrestricted grant (Ipsen Ltd); grant support (rest); *Speaker Bureau:* GSK, Ipsen Ltd, Merz, UCB Pharma, Orion, *Details:* received honoraria for speaking at meetings by the above companies. William Rooney, *Research Support (including provision of equipment or materials):* National Institutes of Health, *Details:* extramural research support, *Ownership Interest:* DeltaPoint Inc, *Details:* start-up company in which I own stock. Penelope Hogarth, *Research Support (including provision of equipment or materials):* 1) Schering Plough Research Institute; 2) Michael J. Fox Foundation, *Details:* 1) research contract paid to my institution for a proof-of-concept study in Parkinson disease;

2) research grant paid to my institution as a participant in a multicenter study, *Consultant:* 1) Schering Plough Research Institute, 2) Apopharma, *Details:* 1) under \$10,000 paid to my institution for consultant services related to Parkinson disease study design; 2) under \$10,000 paid to my institution for my participation in a scientific meeting related to deferiprone use in NBIA. Susan Hayflick, *Research Support (including provision of equipment or materials):* philanthropy.

## References

- McNeill A, Birchall D, Hayflick SJ, et al. T2\* and FSE MRI distinguishes four subtypes of neurodegeneration with brain iron accumulation. *Neurology* 2008;29;70:1614–19
- Yilmaz A, Budak H, Longo R. Paramagnetic contribution of serum iron to the spin-lattice relaxation rate (1/ $\rho_1$ ) determined by MRI. *Appl Magn Reson* 1998;14:51–58
- Burgetova A, Seidl Z, Krasensky J, et al. Multiple sclerosis and the accumulation of iron in the basal ganglia: quantitative assessment of brain iron using MRI T2 relaxometry. *Eur Neurol* 2010;63:136–43
- Miszkiel KA, Paley MN, Wilkinson ID, et al. The measurement of R2, R2\* and R2' in HIV-infected patients using the prime sequence as a measure of brain iron deposition. *Magn Reson Imaging* 1997;15:1113–19
- Waldvogel D, van Gelderen P, Hallett M. Increased iron in the dentate nucleus of patients with Friedrich's ataxia. *Ann Neurol* 1999;46:123–25
- Brar S, Henderson D, Schenck J, et al. Iron accumulation in the substantia nigra of patients with Alzheimer disease and parkinsonism. *Arch Neurol* 2009;66:371–74
- Gerlach M, Ben-Shachar D, Riederer P, et al. Altered brain metabolism of iron as a cause of neurodegenerative diseases? *J Neurochem* 1994;63:793–807
- Kobari M, Nogawa S, Sugimoto Y, et al. Familial idiopathic brain calcification with autosomal dominant inheritance. *Neurology* 1997;48:645–49
- Storey P, Thompson AA, Carqueville CL, et al. R2\* imaging of transfusional iron burden at 3T and comparison with 1.5T. *J Magn Reson Imaging* 2007;25:540–47
- Hallgren B, Sourander P. The Effect of age on the non-haemin iron in the human brain. *J Neurochem* 1958;3:41–51
- Aquino D, Bizzi A, Grisoli M, et al. Age-related iron deposition in the basal ganglia: quantitative analysis in healthy subjects. *Radiology* 2009;252:165–72
- Boddaert N, Le Quan Sang KH, Rötig A, et al. Selective iron chelation in Friedrich ataxia: biologic and clinical implications. *Blood* 2007;110:401–08

13. Hayflick SJ, Penzien JM, Michl W, et al. **Cranial MRI changes may precede symptoms in Hallervorden-Spatz syndrome.** *Pediatr Neurol* 2001;25:166–69
14. Gregory A, Westaway SK, Holm IE, et al. **Neurodegeneration associated with genetic defects in phospholipase A(2).** *Neurology* 2008;71:1402–09
15. Forni GL, Balocco M, Cremonesi L, et al. **Regression of symptoms after selective iron chelation therapy in a case of neurodegeneration with brain iron accumulation.** *Mov Disord* 2008;23:904–07
16. Zhou B, Westaway SK, Levinson B, et al. **A novel pantothenate kinase gene (PANK2) is defective in Hallervorden-Spatz syndrome.** *Nat Genet* 2001;28:345–49
17. Freeman K, Gregory A, Turner A, et al. **Intellectual and adaptive behaviour functioning in pantothenate kinase-associated neurodegeneration.** *J Intellect Disabil Res* 2007;51(pt 6):417–26
18. Kumar N, Boes CJ, Babovic-Vuksanovic D, et al. **The “eye-of-the-tiger” sign is not pathognomonic of the PANK2 mutation.** *Arch Neurol* 2006;63:292–93
19. Kruer MC, Hiken M, Gregory A, et al. **Novel histopathologic findings in molecularly-confirmed pantothenate kinase-associated neurodegeneration.** *Brain* 2011;134(pt 4):947–58
20. Hayflick SJ, Hartman M, Coryell J, et al. **Brain MRI in neurodegeneration with brain iron accumulation with and without PANK2 mutations.** *AJNR Am J Neuroradiol* 2006;27:1230–33
21. Baumeister FA, Auer DP, Hörtnagel K, et al. **The eye-of-the-tiger sign is not a reliable disease marker for Hallervorden-Spatz syndrome.** *Neuropediatrics* 2005;36:221–22
22. Strecker K, Hesse S, Wegner F, et al. **Eye of the tiger sign in multiple system atrophy.** *Eur J Neurol* 2007;14:e1–2
23. Molinuevo JL, Muñoz E, Valdeoriola F, et al. **The eye of the tiger sign in cortical-basal ganglionic degeneration.** *Mov Disord* 1999;14:169–71
24. Morgan NV, Westaway SK, Morton JE, et al. **PLA2G6, encoding a phospholipase A2, is mutated in neurodegenerative disorders with high brain iron.** *Nat Genet* 2006;38:752–54
25. Wild EJ, Mudanohwo EE, Sweeney MG, et al. **Huntington’s disease phenocopies are clinically and genetically heterogeneous.** *Mov Disord* 2008;23:716–20
26. Chinnery PF, Crompton DE, Birchall D, et al. **Clinical features and natural history of neuroferritinopathy caused by the FTLI 460InsA mutation.** *Brain* 2007;130(pt 1):110–19. Epub 2006 Dec 2
27. di Patti MC, Maio N, Rizzo G, et al. **Dominant mutants of ceruloplasmin impair the copper loading machinery in aceruloplasminemia.** *J Biol Chem* 2009;284:4545–54. Epub 2008 Dec 18
28. Merle U, Tuma S, Herrmann T, et al. **Evidence for a critical role of ceruloplasmin oxidase activity in iron metabolism of Wilson disease gene knockout mice.** *J Gastroenterol Hepatol* 2010;25:1144–50
29. Kruer MC, Paisán-Ruiz C, Boddaert N, et al. **Defective FA2H leads to a novel form of neurodegeneration with brain iron accumulation (NBIA).** *Ann Neurol* 2010;68:611–18.
30. Schneider SA, Paisan-Ruiz C, Quinn NP, et al. **ATP13A2 mutations (PARK9) cause neurodegeneration with brain iron accumulation.** *Mov Disord* 2010;25:979–84
31. Behrens MI, Brüggemann N, Chana P, et al. **Clinical spectrum of Kufor-Rakeb syndrome in the Chilean kindred with ATP13A2 mutations.** *Mov Disord* 2010;25:1929–37
32. Alazami AM, Al-Saif A, Al-Semari A, et al. **Mutations in C2orf37, encoding a nucleolar protein, cause hypogonadism, alopecia, diabetes mellitus, mental retardation, and extrapyramidal syndrome.** *Am J Hum Genet* 2008;83:684–91
33. Kuo YM, Hayflick SJ, Gitschier J. **Deprivation of pantothenic acid elicits a movement disorder and azoospermia in a mouse model of pantothenate kinase-associated neurodegeneration.** *J Inherit Metab Dis* 2007;30:310–17
34. Kruer MC, Gregory A, Hogarth P, et al. **Childhood static encephalopathy and cerebral palsy followed by abrupt-onset progressive neurodegeneration in adulthood: a novel neurodegeneration with brain iron accumulation (NBIA) phenotype.** Poster presentations, American Academy of Cerebral Palsy and Developmental Medicine 63rd Annual Meeting, Scottsdale, AZ, September 2009.
35. Hayflick SJ. **Dystonia-parkinsonism disease gene discovery: expect surprises.** *Ann Neurol* 2009;65:2–3
36. Paisan-Ruiz C, Bhatia KP, Li A, et al. **Characterization of PLA2G6 as a locus for dystonia-parkinsonism.** *Ann Neurol* 2009;65:19–23
37. Kurian MA, Morgan NV, MacPherson L, et al. **Phenotypic spectrum of neurodegeneration associated with mutations in the PLA2G6 gene (PLAN).** *Neurology* 2008;70:1623–29
38. Paisán-Ruiz C, Li A, Schneider SA, et al. **Widespread Lewy body and tau accumulation in childhood and adult onset dystonia-parkinsonism cases with PLA2G6 mutations.** *Neurobiol Aging* 2010;33:814–23
39. Galvin JE, Giasson B, Hurtig HI, et al. **Neurodegeneration with brain iron accumulation, type 1 is characterized by alpha-, beta-, and gamma-synuclein neuropathology.** *Am J Pathol* 2000;157:361–68
40. Wakabayashi K, Fukushima T, Koide R, et al. **Juvenile-onset generalized neuroaxonal dystrophy (Hallervorden-Spatz disease) with diffuse neurofibrillary and Lewy body pathology.** *Acta Neuropathol* 2000;99:331–36